1 *Article*

# 2  3  4 Migration of barchan dunes in Qatar – controls of the Shamal, teleconnections, sea-level changes and human impact

5 **Max Engel [1,*], Fabian Boesl [2] and Helmut Brückner [2]**

6  7 [1]  Royal Belgian Institute of Natural Sciences, OD Earth and History of Life, Geological Survey of Belgium, Jennerstraat 13, 1000 Brussels, Belgium

8 [2]  University of Cologne, Institute of Geography, Zülpicher Str. 45, 50923 Cologne, Germany

9 *  Correspondence: max.engel@naturalsciences.be

10

11 **Abstract:** Barchan dune fields are a dominant landscape feature in SE Qatar and a key element of
12 the peninsula's geodiversity. The migration of barchan dunes is mainly controlled by dune size,
13 wind pattern, vegetation cover and human impact. We investigate the variability of dune migration
14 in Qatar over a time period of 50 years using high-resolution satellite and aerial imagery and explore
15 its relation to the regional Shamal wind system, teleconnection patterns, and limitations in sand
16 supply associated with the transgression of the Arabian Gulf. We detect strong size-dependent
17 differences in migration rates of individual dunes as well as significant decadal variability on a
18 dune-field scale, which was found to be correlating with the intensity of the North Atlantic
19 Oscillation (NAO) and the Indian Summer Monsoon (ISM). High uncertainties associated with the
20 extrapolation of migration rates back into the Holocene, however, do not permit to further specify
21 the timing of the loss of sand supply and the onset of the mid-Holocene relative sea-level (RSL)
22 highstand. For the youngest phase considered in this study (2006–2015), human impact is
23 anticipated to have accelerated dune migration under a weakening Shamal regime through sand
24 mining and excessive vehicle frequentation upwind of the core study area.

25 **Keywords:** Aeolian geomorphology; Arabian Peninsula; Arabian/Persian Gulf; Remote sensing;
26 Holocene landscape change

27

## 28 1. Introduction

29 Barchan dunes are singular crescentic features with a convex side directed upwind and two
30 horns pointing downwind. They form from small sand patches by windward deflation over a
31 gradually developing low-angle slope, where grains eventually slide down a steeper leeward slope.
32 This process is faster at the lower margins resulting in the horns running ahead [1]. Barchan dunes
33 form in areas of moderate sand supply and low variability of wind direction [2–4]. Slight variations
34 of wind direction may result in single horn extension or even the transformation to linear dunes [5].
35 Barchan dynamics are complex and their migration is a function of shear stress and, more
36 pragmatically, closely related to wind velocity [2]. Barchans represent excellent recorders of wind
37 pattern changes since migration speed responds sensitively to changes in wind speed by a factor of
38 three [6], even though the secondary, micro-scale air flow regime [2] and dune height play a role as
39 well. Based on the derivate of v (velocity) with respect to u* (wind shear velocity) of Bagnold's [7]
40 equation

$$v = Cu*3/h, \tag{1}$$

41 where C=the constant of proportionality and h=barchan dune height, any modification in wind speed
42 is enhanced by a factor of three in dune velocity [6]. Thus, on a dune field scale, barchan dunes of

43    different sizes may collide and merge [4]. The smallest barchan dunes may reach migration rates of
44    30–100 m yr$^{-1}$ [3]. Speed acceleration and sand transport are highest at the upper part of the gentler
45    windward slope due to upslope streamline compression, whereas the barchan's crest marks the
46    boundary between aeolian erosion and gravitational accumulation areas [2]. Barchan dunes respond
47    to environmental change, as increased moisture and the establishment of vegetation may result in
48    speed reduction or even the transformation into a stationary parabolic or blow-out dune [8].
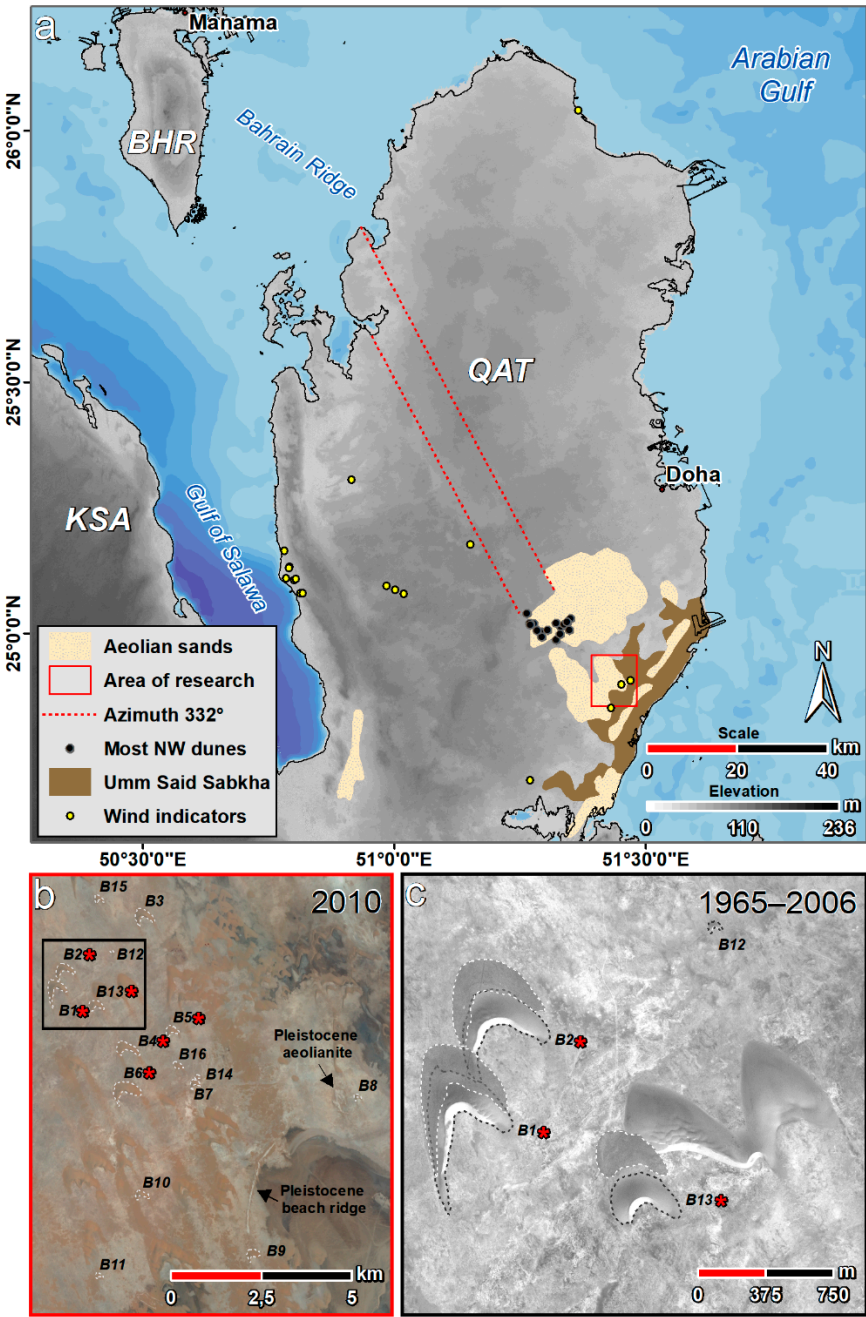


49

**Figure 1.** a) Overview of the Qatar peninsula based on SRTM30 data [9] and the GEBCO_2014 grid
[10] showing the location of the distribution of aeolian surface deposits, the core study area within
the barchan dune fields, the associated downwind Umm Said sabkha, the former main sediment
source areas of the shallow Bahrain Ridge and northern Gulf of Salwa, the main corridor of barchan
migration in the past (azimuth 332° deviation from N after [11]), and the distribution of long-term
geomorphic indicators of Shamal predominance. b) Core study area with barchan dunes B1–B16.
Dunes mined between 2006 and 2015 are marked with red asterisk. c) Examples of dune migration
towards SSE between 1965 (Gambit KH-7) and 2006 (Orbview) (cf. Table 1).
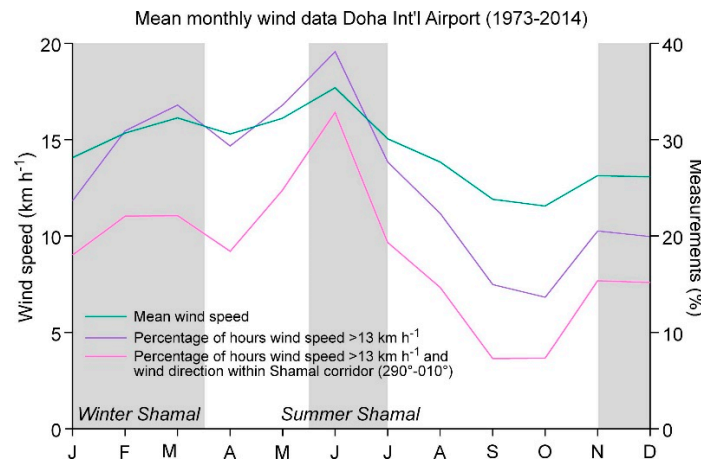
58



**Figure 2.** Monthly distribution of mean wind speed, general percentage of hours of wind speed >13 km h$^{-1}$, and percentage of hours of wind speed >13 km h$^{-1}$ within the Shamal corridor (290°-010° deviation from N) at Doha International Airport [12], the longest serving climate station in Qatar.

Interpolating migration rates from short-term observations is challenging since small dunes may separate from the horns of larger ones [13] and the size of barchans fluctuates over time [4]. Size changes are determined by the difference between upwind sand supply and efflux from the horns, which is a function of horn width [14]. However, on a dune-field scale and in the long term, the size of barchans is considered to stay rather stable [2,15] and, therefore, fluctuations in dune swarm migration over larger time-scales may be closely related to external factors, mostly changing wind patterns or changes in vegetation cover.

In Qatar, remnant barchans dunes occur in the southeast and are assumed to have travelled over the entire peninsula from the NW, driven by the regional Shamal wind regime (Figure 1). Their absence in most parts of Qatar today has been related to rapid post-glacial flooding of the shallow Arabian Gulf starting at around 14,000 years, when mobile sand dunes covered almost the entire floor of the Gulf. At the time when present sea level was reached, shortly before the regional highstand of c. +2 m, sand sources in the wider area of the Bahrain Ridge were drowned resulting in large parts of the peninsula gradually becoming free of dunes [16–18]. The exact timing of the loss of sand supply, however, is largely unclear. Rough estimates of 8000–6000 years ago [19,20], 10,000–8000 years ago [21], or even 12,000 years ago [22] can be found in literature, along with the rather precise timing of 4100 years ago [11]. Likewise, a broad range of dates is found for the mid-Holocene sea-level highstand both in Qatar and the wider Gulf region, e.g. 8000–4000 years ago [23], 5 to 6 millennia ago [24], 6000–4500 cal yrs. BP [25], around 6000 BP [18], 5000–3500 cal yrs. BP [26], or "shortly after 5290–4570 cal yr BP" [27] (p. 79).

In this paper, we provide a precise 50-year record of barchan dune migration in Qatar and analyse the driving mechanisms. Understanding the long-term migration of the peninsula's dunes is important, as their mobility imposes a hazard on built infrastructure and the developing agricultural sector [28]. We discuss the influence of variability in global circulation patterns on Shamal activity and dune mobility. In a further step, we compare extrapolated migration rates with the loss of the sand source after flooding of the Bahrain Ridge and the Gulf of Salwa, and try to provide more precise chronological constraints. In a last step, the effect of human impact through sand mining and excessive vehicle frequentation on barchan dune dynamics in Qatar will be evaluated.

## 2. Study area

*2.1. The physical setting and wind pattern of Qatar*

The Qatar peninsula is an anticlinal structure of uplifted Tertiary limestone, dolomite, marl, chalk and shale formations protruding into the Arabian Gulf. Today's low to moderate relief is formed by the Lower and Middle Eocene Rus and Dammam formations representing shallow marine

95  carbonates with intercalated anhydrites [29, 30]. Tectonic uplift and slight folding since then resulted
96  in the emergence of Qatar, its continental conditions and a lack of sediments from subsequent stages
97  and series. Miocene sedimentary rocks are mainly found in southern Qatar, represented by shallow
98  marine limestones, gypsum, dolomite, and mud of the Dam Formation as well as the continental
99  Hofuf conglomerates. The topography is rather flat, notable rises only occur in the south [29].
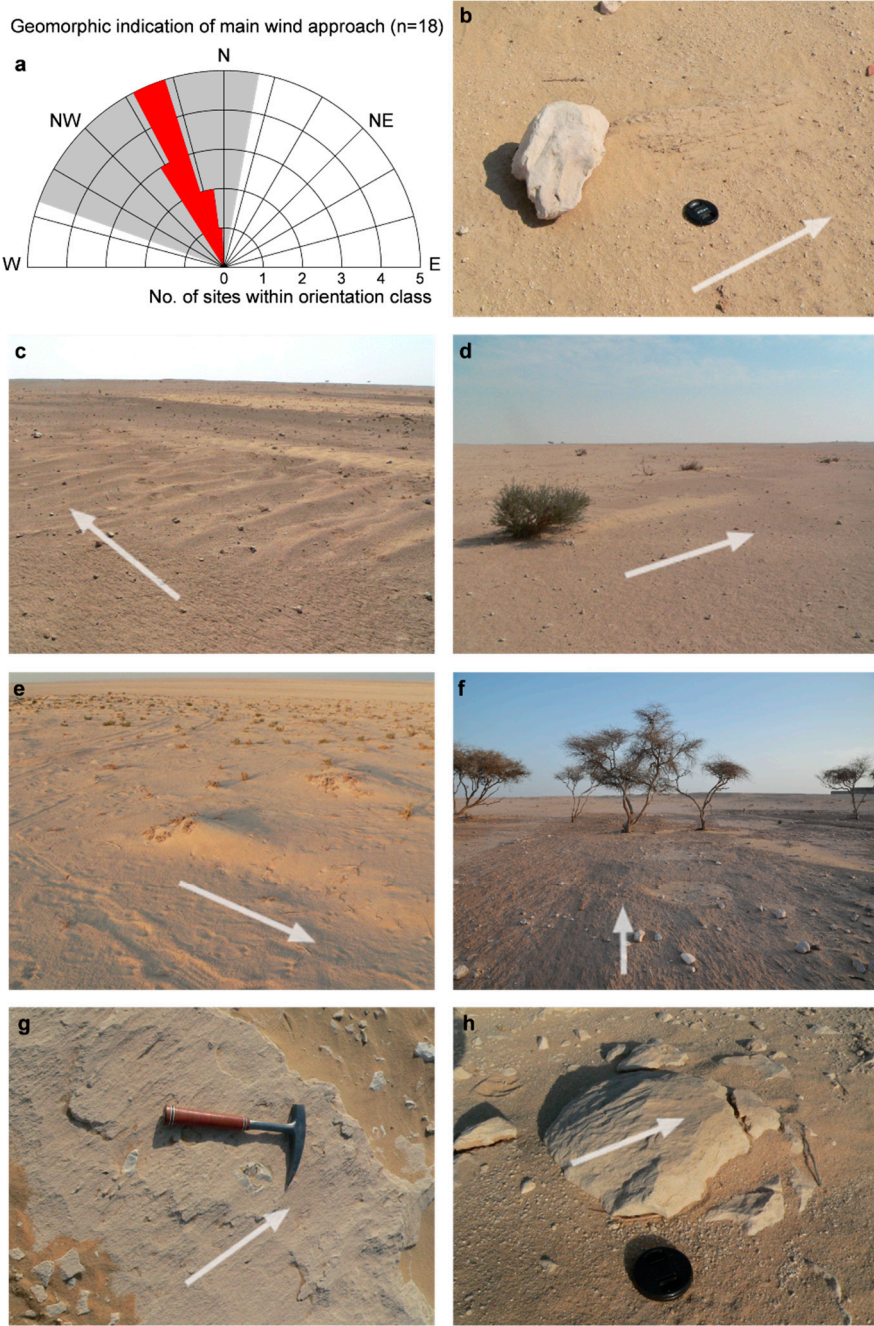


100

101  **Figure 3**. a) Direction of all geomorphic indicators of Shamal predominance mapped during the field
102  survey (Figure 1a). The wider Shamal of 290°–010° is grey-shaded. b) Micro-yardang inside a *rawdha*
103  indicating deflation in these silt/sand-filled karstic depressions. Its formation is triggered by
104  protection through a larger boulder. c) Transversal wind ripples perpendicular to Shamal direction,
105  c. 10 cm high. d) Incipient nebkha associated with a rather long drape of sand developed in the lee of
106  a shrub. e) Small herbaceous nebkha with shorter leeward tail. f) Linear corrasion features on a *rawdha*
107  surface. g) Linear corrasion features on a MIS 5 beachrock (see "Pleistocene beach ridge" in Figure 1b)
108  [25]. h) Linear corrasion features on subarially exposed Dammam limestone. All arrows point into the
109  downwind Shamal direction.

110    The climate of Qatar is arid, though the relative humidity may rise up to 90%. The annual
111    precipitation ranges between 50–80 mm and occurs mainly during winter and spring (Figure 2).
112    However, the spatio-temporal pattern of rainfall is very irregular [11]. The wind regime is dominated
113    by the NW to N regional Shamal winds, approaching Qatar mostly during early June to mid-July and
114    November to March, respectively [31]. This regional wind system mostly affects Saudi Arabia,
115    Kuwait, and Qatar [32] and controls the movement of barchans in SE Qatar [11]. In May, the summer
116    Shamal is mainly determined by a lower to middle tropospheric westerly trough over Iran and a
117    corresponding ridge over Anatolia resulting in atmospheric descent over the northern Arabian
118    Peninsula and creation of a regional high, which, in combination with an established low over Iran,
119    initiates short-term, multiple-day Shamal conditions over Qatar [32]. Surface wind speeds reach up
120    to 13 m s$^{-1}$ [33]. Stronger and longer-duration Shamals during June and July are controlled by a steep
121    gradient between the Mediterranean high-pressure cell, and the regional low over Iran resulting from
122    extreme heating of surface air masses [32,34,35]. The winter Shamal (November to March) may even
123    reach wind speeds of 15–20 m s$^{-1}$ over the Arabian Gulf [35,36] and is usually associated with a surface
124    low-pressure area over Syria migrating eastward towards Iran and pushing a cold front south and
125    west. A low along this southward moving front in the northern Arabian Gulf and a surface high over
126    the northern Arabian Peninsula finally induce the winter Shamal, which is not as consistent as its
127    summer counterpart [31]. The long-term persistence of dominating winds from 290–010° is also
128    reflected by the alignment of the main axis of nebkhas and sand drapes at prehistoric burial cairns,
129    by micro-yardangs inside the inland sediment-filled depressions (*rawdhat*), or sandblasting features
130    on rock surfaces in most parts of the peninsula (Figure 3).

131    *2.2. Barchans of Qatar*

132    Barchanoid dunes cover significant parts of the ergs of the Sahara, the Takla Makan in northern
133    China, the Pesky Karakumy of Kasakhztan and the Rub' al-Khali on the eastern Arabian Peninsula
134    [37]. In Qatar, dunes are concentrated in the southeast and cover c. 10% of the entire peninsula, i.e. c.
135    976 km². According to the main approaching angle of the Shamal winds, the tails of the barchans
136    point to SSE–SE [11,29]. Embabi and Ashour [11] mapped four types of barchans dunes in SE Qatar,
137    including (i) textbook-like simple barchans of various sizes (width across horns 15–1000 m); (ii)
138    modified barchans with a longer and thinner western horn; (iii) compound barchans in transition to
139    longitudinal dunes; and (iv) fully developed longitudinal dunes. Dune asymmetry as observed
140    within the modified barchans is ascribed to a local SE wind component. Height reaches up to 40 m
141    but is mostly less than 10 m. The barchans mainly consist of quartz sand with minor portions of
142    skeletal grains and dust with occasional heavy mineral components, locating its source on the
143    Arabian Shield. Sands are unimodal and peak in fine to medium classes. Grains are generally
144    rounded to subrounded [11]. Barchan dunes covering the floor of the shallow Gulf of Salwa have also
145    been identified on Landsat imagery [21].

146    **3. Materials and methods**

147    In a first step, the migration was recorded for 16 individual barchan dunes (B1–B16) by
148    multitemporal analysis of high-resolution satellite images. The study area was defined based on the
149    availability on satellite scenes, and the presence and traceability of barchan dunes. The multitemporal
150    analyses included Gambit KH-7 (1965), Hexagon KH-9 (1978), a resampled aerial ortho-mosaic (1995),
151    Orbview (2006), and SPOT (2015) data (Table 1). All scenes were rectified using an IKONOS mosaic
152    of 2004 and 40–60 reference points by spline transformation/interpolation in ArcGIS. The IKONOS
153    scene uses the local coordinate reference system QND95 and is projected on the Qatar National Grid.
154    Some of the few persistent reference features are provided by Pleistocene aeolianite and beachrock
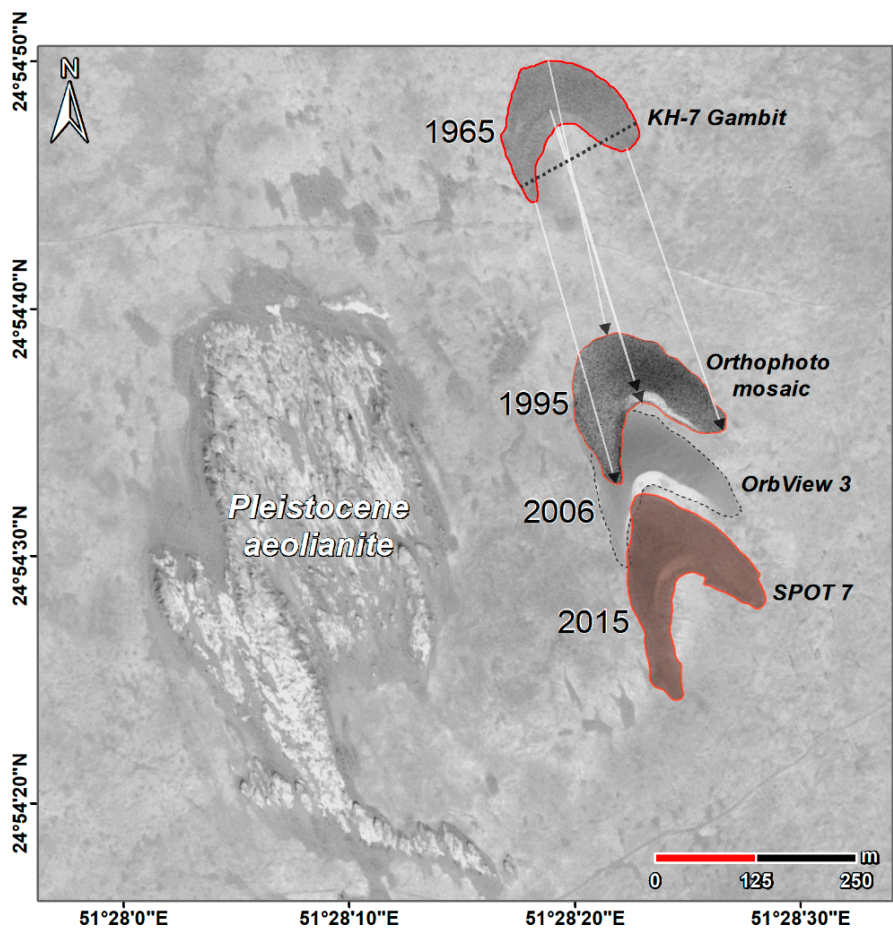155    in an otherwise highly dynamic landscape (Figure 1b).

**Figure 4.** Approach of multitemporal satellite and aerial image analysis exemplified for barchan dune B8 (Figure 1b). Between 1965 and 2015, the entire barchan moved for ca. 587 m towards SSE (average value), the western horn even 636 m.

**Table 1.** Imagery used in this study.

| Mission | Date | Resolution | Remarks | Application |
|---|---|---|---|---|
| Gambit (KH-7) | 04 Nov 1965 | c. 0.6–1.2 m/pixel | 0.8 m/pixel in the used scene | 50-year analysis of dune migration; comparison dry/moist surface |
| Hexagon (KH-9) | 03 Apr 1978 | c. 6–9 m/pixel | Resolution insufficient for study | - |
| Aerial ortho-mosaic | Feb 1995 | 1 m/pixel | Sampled to 1 m/pixel | 50-year analysis of dune migration |
| IKONOS | 2004 | 1 m/pixel | First commercial satellite to reach 1 m/pixel; color | Ortho-rectification; comparison dry/moist surface |
| OrbView-3 | 04 Mar 2006 | c. 1 m/pixel | 1 m/pixel in the used scene | 50-year analysis of dune migration |
| SPOT 7 | 04 May 2015 | c. 1.5 m/pixel | 1.7 m/pixel in the used scene, color | 50-year analysis of dune migration |

The migration was defined as the average displacement of five different reference points on the dune per number of months in between two images: the intersection of the crest as well as the windward and leeward boundaries with the centerline axis, and the tips of both horns (Figure 4). The width across both horns is the main size measure based on the linear relationship between dune height and horn-to-horn width [5,15]. Considering a range of global datasets, Hesp and Hastings [5] express this relationship as

$$w=8.82h+7.65, \tag{2}$$

167 where w=horn-to-horn width, and h=height of the barchan slip face ($R^2$=0.808). This type of manual
168 measurement of dune migration for high-resolution imagery in the range of 1 m/pixel has provided
169 reliable results comparable to those from the application of automated tools of subpixel correlation
170 of satellite imagery, such as COSI-Corr [6]. The Hexagon imagery from 1978, however, was
171 eventually discarded due to insufficient resolution, while for the SPOT imagery, individual dunes
172 had to be discarded due to extensive mining activities after 2006 (Figure 5).

173 The influence of bottom moisture on the migration rate was tested by comparison of additional four
174 pairs of barchan dunes of similar sizes, each pair comprising one dune from the Umm Said sabkha
175 with very shallow, fluctuating groundwater levels of only a few tens of cm below surface [28], and
176 one travelling over entirely dry Dammam limestone.

177 In order to estimate the time when the Bahrain Ridge and the Gulf of Salwa became flooded,
178 current relative sea level was reached, and the sand source became cut off, we measured travel times
179 of the 15 barchan dunes within the width range 100–500 m closest to the NW coast (<80 km). The
180 distance to the NW coast was measured in the main Shamal azimuth of 332° deviation from N [11],
181 while individual, size-dependent migration velocities were derived from the regression function of
182 our empirical dataset established in the first step (eq. 4). For interpretation, individual travel times of
183 the barchans from today's shoreline to their present position were transformed into a probability
184 density function (PDF). An error of 10% and a normal probability distribution were assumed for each
185 time value (=mean value), from which probabilities for additional 20 time values in 1% steps starting
186 from the mean value were derived (-10% to +10%), resulting in 315 data points in total. Binning of the
187 time axis starts at $x_0$=100 and follows the equation
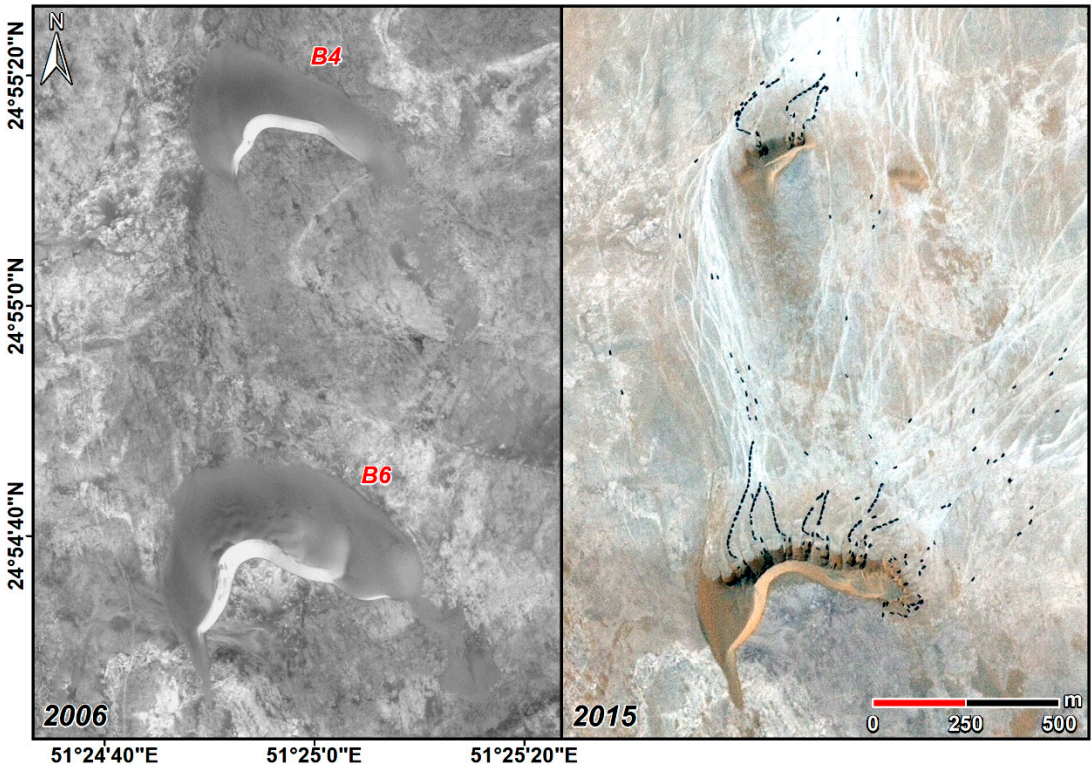
$$x=x_0+x_0/100. \tag{3}$$

188



189 **Figure 5**. Documentation of Sand mining at two dunes of the core study area between 2006 and 2015
190 as well as associated massive frequentation of >100 heavy trucks at a time, which access the NW part
191 of the core study area from the upwind corridor.

192    **4. Results**

193    *4.1. Barchan migration*

194    The migration rate of the 16 investigated barchan dunes between 1965 and 2006 varies greatly
195    (Figure 6a) ranging from 177 m for a width of 580 m to 951 m (B1) for a width of 74 m (B12). A
196    significant inverse power-law relationship with a confidence of $R^2=0.86$ can be stated for the size-
197    distance distribution following the function

$$\ln(Y)=-1.12*\ln(X)+5.23, \tag{4}$$

198    where Y=horn-to-horn width (m) and X=migration distance per month (m).
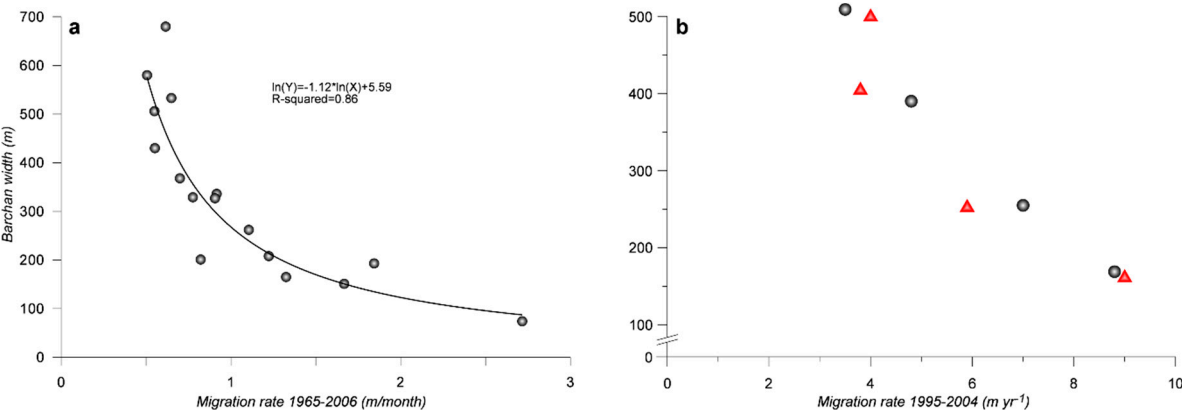


199

200    **Figure 6**. a) Relationship between size of barchan dunes B1–B16 and migration rate over the time
201    period 1965–2006, which is best explained by an inverse power-law function. b) Comparison of
202    migration rates between pairs of similarly sized dunes migrating over dry Dammam limestone
203    surface (circles) and moist sabkha surface (triangles).

204    In order to investigate whether surface moisture has an influence on migration rates, pairs of
205    dunes of similar size travelling over dry Dammam limestone and the Umm Said sabkha with a
206    groundwater table of only a few dm [29] were compared (Figure 6b). While the smallest pair of
207    barchan dunes travelled at comparable speed, the two medium-sized dunes show a slightly faster
208    rate on dry ground. When comparing the largest dunes of the sample, the one inside the sabkha
209    migrates faster. In general, no clear pattern can be observed.
210    Highest dune migration rates were inferred for the time window 1965–1995 ranging from 0.4
211    m/month (B1) to 2.1 m/month (B12) (Figure 7f). The time window 1995–2006 witnesses a significant
212    drop without exception to migration rates of 0.3 m/month to 1.7 m/month. In turn, among the ten
213    barchan dunes not mined between 2006 and 2015, only the largest one became slower (from 0.3 to 0.1
214    m/month). All other dunes experienced an increased migration rate to levels generally below the
215    period 1965–1995 (Figure 7e).

216    The travel times of the barchan dune population in closest proximity to the NW coast (by
217    considering the main Shamal azimuth after Embabi and Ashour [11]), which are assumed to coincide
218    with the cut-off of the sand source and the onset of the mid-Holocene highstand, are deduced from
219    eq. 4 and vary greatly (Figure 8). This large discrepancy is due to the significant size dependency of
220    migration rates. The PDF covers the time period between 3300 and almost 17,000 yrs BP with a small
221    gap around 10,300 yrs BP.

222    *4.2. Shamal activity*

223    In terms of further mechanisms controlling barchan migration in the longer term, a significant
224    correlation between regional (number of summer Shamal days over the Gulf region, Figure 7b) and
225    local (average wind speed June-July at Doha International Airport, Figure 7c) summer Shamal

226  activity can be observed. From the 1970s until today, the summer Shamal constantly declined, with a
227  clear step in the mid-1990s (Figure 7b,c). Likewise, if considering the time windows of the
228  multitemporal satellite image analysis of barchan dune migration, the duration of Shamal conditions
229  has dropped from 21.5% (1973–1995) to 15.2% (1995–2006) and 14.8% (2006–2015) (Figure 7e). The
230  positive relationship between the North Atlantic Oscillation (NAO) and the Shamal activity is evident
231  over the longer term, as the intensity of the NAO also declined over the last decades. In particular
232  years of positive or negative summer Shamal extremes in Qatar, such as in 1980/1981, 1983, 1993,
233  2000, or 2013, show the NAO dependency (Figures 7c,d). Likewise, it seems that the intensity of the
234  Indian Summer Monsoon (ISM) reveals similarities with Shamal activity, as exemplified for the
235  strong Shamal years of 1994 and 2015, or the calmer Shamal phase after 1995 (Figure 7a).

## 5. Discussion

237       The multitemporal analysis of satellite imagery revealed the well-established pattern of size-
238  dependent migration rates of barchan dunes [14,15]. However, over centennial and millennial scales,
239  barchan size may vary significantly [4,13] potentially leading to uncertainty when extrapolating such
240  rates.
241       On a dune-field scale, Shamal activity is the main control of barchan migration in Qatar, as
242  shown by remote sensing data from 1965–2006. Surface moisture variability is considered negligible
243  based on investigation of the sbakha/non-sabkha couplets. As it coincides with driest conditions over
244  the year, the summer Shamal is most efficient in terms of particle transport in the Middle East [36,40].
245  The dependency of the summer Shamal activity from teleconnection patterns is evident from the
246  positive relationship between the NAO index and average wind speed measured at Doha
247  International Airport. This relationship may be explained by the NAO controlling the intensity of the
248  summer season stationary high over the Eastern Mediterranean [41]. The Shamal is fuelled by a steep
249  gradient between the Mediterranean high-pressure cell and the low associated with the ISM located
250  over NW India, Iran, Iraq, Pakistan, and Afghanistan [36,42,43]. This low pressure area usually forms
251  in May and emanates from intense surface heating. It is closely associated with both the upper level
252  mid-latitude circulation over western central Asia and low-level monsoonal circulation over the
253  Arabian Sea and the Indian subcontinent [42,44].
254       The NAO and the ISM have been active over the entire Holocene to support the Shamal and
255  dune migration over the Qatar peninsula, even though both mechanisms show a gradual weakening
256  trend over the Holocene in response to solar insolation [45,46]. In their exhaustive analysis on
257  Quaternary stratigraphy and environments of the Arabian Peninsula, Glennie and Singhvi [47]
258  confirm the long-term persistence of the Shamal, but state a generally weaker intensity during
259  interglacials. While decreasing trends of the NAO and the ISM may indicate a Shamal stronger than
260  today over most of the Holocene and, hence, higher migration rates, wetter conditions during the
261  early to mid-Holocene transition identified in many parts of the Arabian Peninsula [46,48–50] may
262  have stimulated vegetation cover slowing down sand flux and migration speed [4,8,51,52]. In what
263  way these competing mechanisms led to deviations from the migration rates identified in the shorter
264  term multitemporal satellite and aerial image analysis of this study over millennial time scales
265  remains a matter of speculation.
266       During the period 2006–2015 the pattern of dune migration significantly deviates, i.e. a speed
267  increase is accompanied by a weakening of ISM, NAO, and, thus, Shamal activity (Figure 7e). As
268  different varieties of human impact can have tremendous influence on dune mobility – mostly,
269  however, through interaction with vegetation [34,53] –, we hypothesize that the intense sand mining
270  activities in the NW part of the core study area have changed the local wind field and significantly
271  increased sand flux, in particular in the lower range of the dune-forming grain-size spectrum. Both
272  massive truck traffic upwind of the core study area (Figure 5) [54] and the sand mining process itself
273  are assumed to have strongly stimulated sand flux, which is correlated to downwind barchan velocity
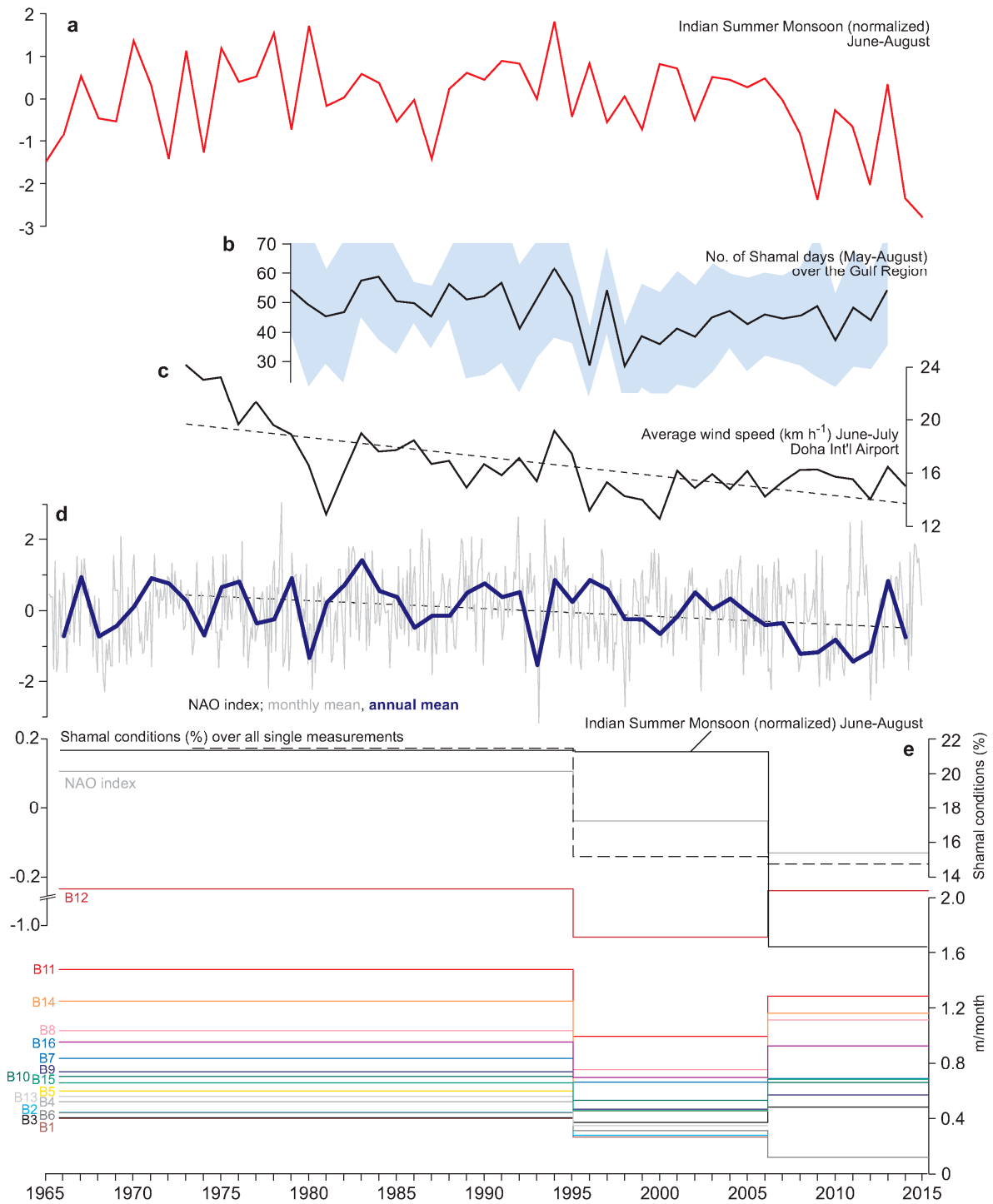274  [6,7].

**Figure 7**. a) Index of Indian Summer Monsoon (ISM) intensity between June and August after Wang and Fan [38]. b) Number of annual Shamal days between May and August over the entire Gulf region. The shading indicates the ±1σ standard deviation across all stations considered [36]. c) Average wind speed in the months of June and July measured at Doha International Airport [12]. d) Monthly and annual mean of the North Atlantic Oscillation (NAO) index, representing the difference between the normalized mean winter air pressure at sea level between Lisbon, Portugal (Azores High), and Stykkisholmur, Iceland (Icelandic Low) [39]. e) ISM, NAO and the percentage of Shamal conditions in Qatar averaged over the time windows of the multitemporal satellite and aerial image analysis of barchan dune migration. These data are displayed in combination with migration rates of barchan dunes B1–B16.
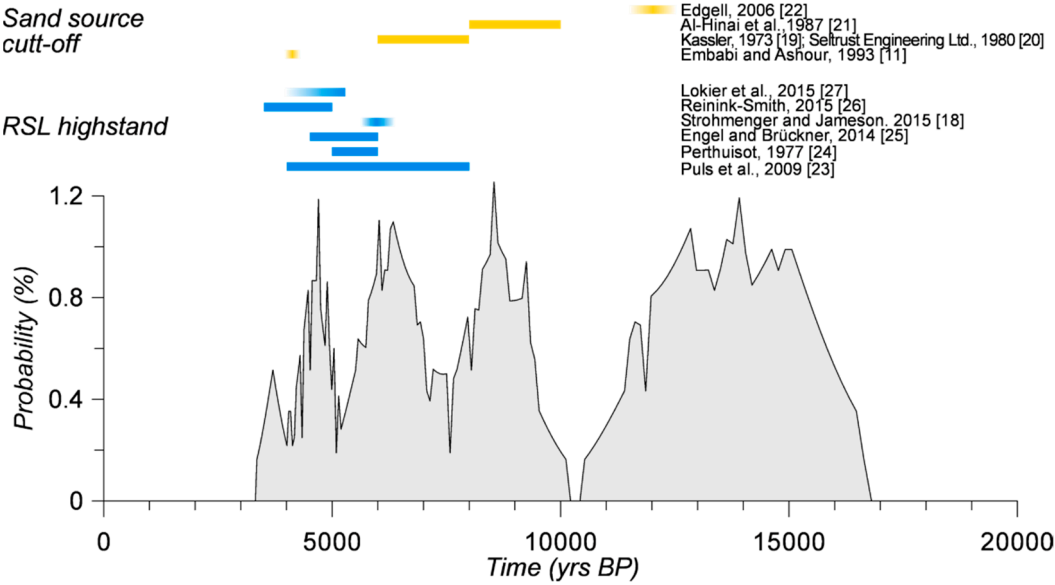
286

**Figure 8**. Probability density function of travel times of the 15 barchan dunes (width 100–500 m) of SE Qatar in closest proximity to the NW coast (Figure 1a). Data are displayed in combination with chronological estimates of the relative sea-level (RSL) highstand (blue bars) and the loss of the sand source (yellow bars) as inferred from literature.

Due to the large size-dependent differences in migration rates of the most NW dunes, the PDF of inferred travel times shows a very broad distribution ranging from c. 3300 to 17,000 yrs BP. Neither does this result conflict with any of the chronological estimates for the mid-Holocene RSL highstand and the loss of the sediment source (Figure 8), nor, unfortunately, does it add more precision to the debate. It can be stated, however, that the loss of the sand source associated with the transgression of the Gulf is to be chronologically located near the younger end of the PDF distribution, most likely between 8000–6000 yrs. BP, as estimated by Kassler [19] and Seltrust Engineering Ltd. [20]. Taking into account the range of estimates for the mid-Holocene RSL highstand with the highest overlap between the different sources (c. 6000–4000 yrs. BP, Figure 8), the estimates of 10,000–8000 yrs. BP [21] and 12,000 yrs. BP [22] are too early, as much of the very shallow wider Bahrain Ridge area was definitely still exposed. The estimate of 4100 yrs. BP [11], however, is too young, as it post-dates the vast majority of known index points of the RSL highstand along the southern coast of the Arabian Gulf [18,25,27]. Inferences from the analysis of Embabi and Ashour [11] might have been biased by the very short time windows of available imagery and the overrepresentation of very small barchans.

## 6. Conclusions

The Shamal wind system is the main driver of barchan dune migration in Qatar. The distribution of the remaining major barchan dune population in the SE of the peninsula in combination with the strongly size-dependent migration rates inferred from multitemporal satellite and aerial image analysis support the hypothesis of a RSL-controlled sediment supply. Due to large uncertainties associated with extrapolation of migration rates into millennial time scales, however, no further chronological constraints can be made regarding the loss of the sand source.

It is shown that the barchan-moving Shamal correlates with two major modules of the global atmospheric circulation, i.e. the North Atlantic Oscillation (NAO) and the Indian Summer Monsoon (ISM). Both systems, though fluctuating, were clearly established over Holocene time scales [45,46], and so was the Shamal [47].

The correlation between Shamal activity and the velocity of barchan dunes comes to an abrupt end after the onset of sand mining in the core study area after 2006. We hypothesize that excessive truck traffic upwind and sand loading at the mined barchan dunes strongly increased sand flux and, thus, downwind migration velocity, representing a rather dramatic example of human interference

320  with the dynamics of dune systems. According to past and present migration rates, the iconic barchan
321  dune landscape of Qatar will still be present for centuries, even if not millennia. However, it seems
322  that the size of this important geo-heritage will shrink much faster due to human activity – directly
323  through sand mining, and indirectly through strongly increased migration rates leading to faster
324  calving into the shallow waters off the SE coast of Qatar, where the sand feeds the extensive Umm
325  Said coastal sabkha system.

333  **Author Contributions:** M.E. conceived and designed the study; F.B. performed the investigations on satellite
334  imagery; all authors analyzed the data; M.E. wrote the manuscript; all authors commented on and approved the
335  manuscript.

336  **Conflicts of Interest:** The authors declare no conflict of interest.

## References

338  1.    Besler, H. Eine Wanderdüne als Soliton? *Phys. Bl.* **1997**, *53*, 983–985, DOI:10.1002/phbl.19970531009.
339  2.    Livingstone, I.; Wiggs, G.F.S.; Weaver, C.M. Geomorphology of desert sand dunes: A review of recent
340        progress. *Earth Sci. Rev.* **2007**, *80*, 239–257, DOI:10.1016/j.earscirev.2006.09.004.
341  3.    Parteli, E.J.R.; Durán, O.; Herrmann, H.J. Minimal size of a barchan dune. *Phys. Rev. E* **2007**, *75*, 011301,
342        DOI:10.1103/PhysRevE.75.011301.
343  4.    Wiggs, G.F.S. Dune morphology and dynamics. In *Treatise in Geomorphology, Vol. 11: Aeolian Geomorphology*;
344        Lancaster, N., Sherman, D.J., Baas, A.C.W., Eds.; Academic Press, London, UK, 2013; pp. 201–218,
345        DOI:10.1016/B978-0-12-374739-6.00304-3.
346  5.    Hesp, P.A.; Hastings, K. Width, height and slope relationships and aerodynamic maintenance of barchans.
347        *Geomorphology* **1998**, *22*, 193–204, DOI:10.1016/S0169-555X(97)00070-6.
348  6.    Vermeesch, P.; Leprince, S. A 45-year time series of dune mobility indicating constant windiness over the
349        central Sahara. *Geophys. Res. Lett.* **2012**, *39*, L14401, DOI:10.1029/2012GL052592.
350  7.    Bagnold, R.A. *The Physics of Blown Sand and Desert Dunes*. Methuen, London, UK, 1941.
351  8.    Bubenzer, O.; Besler, H. Sands as Archives of Environmental Change: Examples from Egypt, Sudan and
352        Namibia. In *Towards Interdisciplinarity – Experiences of the Long-term ACACIA Project*; Möhlig, W.J.G.,
353        Bubenzer, O., Menz, G., Eds.; Rüdiger Köppe Verlag, Cologne, Germany, 2010; pp. 23–48
354  9.    Farr, T.G.; Rosen, P.A.; Caro, E.; Crippen, R.; Duren, R.; Hensley, S.; Kobrick, M.; Paller, M.; Rodriguez, E.;
355        Roth, L.; Seal, D.; Shaffer, S.; Shimada, J.; Umland, J.; Werner, M.; Oskin, M.; Burbank, D.; Alsdorf, D. The
356        Shuttle Radar Topography Mission. *Rev. Geophys.* **2007**, *45*, RG2004, DOI:10.1029/2005RG000183.
357  10.  Weatherall, P.; Marks, K.M.; Jakobsson, M.; Schmitt, T.; Tani, S.; Arndt, J.E.; Rovere, M.; Chayes, D.; Ferrini,
358        V.; Wigley, R. A new digital bathymetric model of the world's oceans. *Earth Space Sci.* **2015**, *2*, 331–345,
359        DOI:10.1002/2015EA000107.
360  11.  Embabi, N.S.; Ashour, M.M. Barchan dunes in Qatar. *J. Arid Environ.* **1993**, *25*, 49–69,
361        DOI:10.1006/jare.1993.1042.
362  12.  NCDC (National Climate Data Center). NOAA NCDC Climate Data Online. URL:
363        https://www7.ncdc.noaa.gov/CDO/, last access: 12 Nov 2017.
364  13.  Anderson, R.S. The attraction of sand dunes. *Nature* **1996**, *379*, 24–25, DOI:10.1038/379024a0.
365  14.  Hersen, P.; Andersen, K.H.; Elbelrhiti, H.; Andreotti, B.; Claudin, P.; Douady, S. Corridors of barchan
366        dunes: stability and size selection. *Phys. Rev. E* **2004**, *69*, 011304, DOI:10.1103/PhysRevE.69.011304.
367  15.  Hesse, R. Do swarms of migrating barchan dunes record paleoenvironmental changes? — A case study
368        spanning the middle to late Holocene in the Pampa de Jaguay, southern Peru. *Geomorphology* **2009**, *104*,
369        185–190, DOI:10.1016/j.geomorph.2008.08.006.

16. Shinn, E.A. Carbonate coastal accretion in the area of longshore transport, NE Qatar. In *The Persian Gulf: Holocene Carbonate Sedimentation and Diagenesis in a Shallow Epicontinental Sea*; Purser, B.H., Ed.; Springer, Berlin, Germany, 1973; pp. 179–191, DOI:10.1007/978-3-642-65545-6_10.

17. Glennie, K.W.; Singhvi, A.K. Event stratigraphy, paleoenvironment and chronology of SE Arabian deserts. *Quat. Sci. Rev.* **2002**, *21*, 853–869. DOI:10.1016/S0277-3791(01)00133-0.

18. Strohmenger, C.J.; Jameson, J. Modern coastal systems of Qatar as analogues for arid climate carbonate reservoirs: improving geological and reservoir modelling. *First Break* **2015**, *33*, 41–50, DOI:10.3997/1365-2397.2014027.

19. Kassler, P. The structural and geomorphic evolution of the Persian Gulf. In *The Persian Gulf: Holocene Carbonate Sedimentation and Diagenesis in a Shallow Epicontinental Sea*; Purser, B.H., Ed.; Springer, Berlin, Germany, 1973; pp. 11–32, DOI: 10.1007/978-3-642-65545-6_2.

20. Seltrust Engineering Ltd. *Qatar Geological Map, scales 1:100,000 (four sheets) and 1:200,000 (one sheet) and explanatory booklet*. IDTC., Doha, Qatar, 1980; 20 p.

21. Al-Hinai, K.G.; McMahon Moore, J.; Bush, P.R. LANDSAT image enhancement study of possible submerged sand-dunes in the Arabian Gulf. *Int. J. Remote Sens.* **1987**, *8*, 251–258, DOI:10.1080/01431168708948639.

22. Edgell, H.S. *Arabian Deserts – Nature, Origin, and Evolution*. Springer: Dordrecht, The Netherlands, 2006; pp. 187–188, DOI:10.1007/1-4020-3970-0.

23. Puls, D.D.; Jameson, J.; Kozar, M.; Al-Ansi, H.; LeBlanc, J. The Dukhan Sabkha: A Modern Analog for the Arab C Carbonate Reservoir, Dukhan Field, Qatar. In Proceedings of the International Petroleum Technology Conference, Doha, Qatar, 7–9 December 2009, Vol. 3; pp. 1799–1811, DOI:10.2523/IPTC-13629-MS.

24. Perthuisot, J.P. Contribution a l'étude du Quaternaire marin de la péninsule de Qatar. *Bull. Soc. Géol. France* **1977**, *S7-XIX*, 1167–1170, DOI:10.2113/gssgfbull.S7-XIX.5.1167.

25. Engel, M.; Brückner, H. The South Qatar Survey Project (SQSP) – Preliminary findings on Holocene coastal changes and geoarchaeological archives. *Z. Orient Archäol.* **2014**, *7*, 290–301.

26. Reinink-Smith, L.M. AMS-dated mollusks in beach ridges and berms document Holocene sea-level and coastal changes in northeastern Kuwait Bay. *Quat. Res.* **2015**, *87*, 200–213, DOI:10.1016/j.yqres.2015.06.005.

27. Lokier, S.W.; Bateman, M.D.; Larkin, N.R.; Rye, P.; Stewart, J.R. Late Quaternary sea-level changes of the Persian Gulf. *Quat. Res.* **2015**, *84*, 69–81, DOI: 10.1016/j.yqres.2015.04.007.

28. Sadiq, A.; Hoqari, F. Remote sensing and spectral characteristics of desert sand from Qatar Peninsula, Arabian/Persian Gulf. *Remote Sens.* **2009**, *1*, 915–933, DOI:10.3390/rs1040915.

29. Al-Yousef, M. Mineralogy, Geochemistry and the origin of Quaternary sabkhas in the Qatar Peninsula, Arabian Gulf. PhD thesis, Faculty of Earth Sciences, University of Southampton, 2003.

30. Al-Saad, H. Lithostratigraphy of the Middle Eocene Dammam Formation in Qatar, Arabian Gulf: Effects of sea-level fluctuations along a tidal environment. *J. Asian Earth Sci.* **2005**, *25*, 781–789, DOI:10.1016/j.jseaes.2004.07.009.

31. Rao, P.G.; Al-Sulaiti, M.; Al-Mulla, A.H. Winter shamals in Qatar, Arabian Gulf. *Weather* **2001**, *56*, 444–451, DOI:10.1002/j.1477-8696.2001.tb06528.x

32. Rao, P.G.; Hatwar, H.R.; Al-Sulaiti, M.H.; Al-Mulla, A.H. Summer shamals over the Arabian Gulf. *Weather* **2003**, *58*, 471–478, DOI:10.1002/wea.6080581207.

33. Bartlett, K.S. Dust Storm Forecasting for Al Udeid AB, Qatar: An Empirical Analysis. MSc thesis, Air University, Ohio, 2004.

34. Barth, H.-J. Characteristics of the wind regime north of Jubail, Saudi Arabia, based on high resolution wind data. *J. Arid Environ.* **2001**, *47*, 387–402, DOI:10.1006/jare.2000.0668.

35. Yu, Y.; Notaro, M.; Kalashnikova, O.V.; Garay, M.J. Climatology of summer Shamal wind in the Middle East. *J. Geophys. Res.-Atmos.* **2016**, *121*, 289–305, DOI:10.1002/2015JD024063.

36. Al Senafi, F.; Anis, A. Shamals and climate variability in the Northern Arabian/Persian Gulf from 1973 to 2012. *Int. J. Climatol.* **2015**, *35*, 4509–4528, DOI:10.1002/joc.4302.

37. Breed, C.S.; Grow, T., 1979. Morphology and distribution of dunes in sand seas observed by remote sensing. In: McKee, E.D. (ed.), A study of global sand seas. *Geol. Surv. Prof. Paper* **1979**, *1052*, 253–304.

38. Wang, B.; Fan, Z. Choice of South Asian Summer Monsoon Indices. *Bull. Amer. Meteor. Soc.* **1999**, *80*, 629–638, DOI:10.1175/1520-0477(1999)080<0629:COSASM>2.0.CO;2.

423   39.   NWS (National Weather Service). North Atlantic Oscillation (NAO). URL:
424         http://www.cpc.ncep.noaa.gov/data/teledoc/nao.shtml, last access 16 April 2018.
425   40.   Middleton, N.J. A geography of dust storms in Southwest Asia, *Int. J. Climatol.* **1986**, *6*, 183–196,
426         DOI:10.1002/joc.3370060207.
427   41.   Ben-Gai, T.; Bitan, A.; Manes, A.; Alpert, P.; Kushnir, Y. Temperature and surface pressure anomalies in
428         Israel and the North Atlantic Oscillation. *Theor. Appl. Climatol.* **2001**, *69*, 171–177,
429         DOI:10.1007/s007040170023.
430   42.   Saeed, S.; Müller, W.A.; Hagemann, S.; Jacob, D. Circumglobal wave train and the summer monsoon over
431         northwestern India and Pakistan: the explicit role of the surface heat low. *Clim. Dyn.* **2011**, *37*, 1045–1060,
432         DOI:10.1007/s00382-010-0888-x.
433   43.   Hamidi, M.; Kavianpour, M.R.; Shao, Y. Synoptic analysis of dust storms in the Middle East. *Asia-Pacific J.*
434         *Atmos. Sci.* **2013**, *49*, 279–286, DOI:10.1007/s13143-013-0027-9.
435   44.   Bansod, S.D.; Singh, S.V. Pre-monsoon surface pressure and summer monsoon rainfall over India. *Theor.*
436         *Appl. Climatol.* **1995**, *51*, 59–66, DOI:10.1007/BF00865540.
437   45.   Rimbu, N.; Lohmann, G.; Kim, J.-H.; Arz, H.W.; Schneider, R. Arctic/North Atlantic Oscillation signature
438         in Holocene sea surface temperature trends as obtained from alkenone data, *Geophys. Res. Lett.* **2003**, *30*,
439         1280, DOI:10.1029/2002GL016570.
440   46.   Fleitmann, D.; Burns, S.J.; Mangini, A.; Mudelsee, M.; Kramers, J.; Villa, I.; Neff, U.; Al-Subbary, A.A.;
441         Buettner, A.; Hippler, D.; Matter, A. Holocene ITCZ and Indian monsoon dynamics recorded in stalagmites
442         from Oman and Yemen (Socotra). *Quat. Sci. Rev.* **2007**, *26*, 170–188, DOI:10.1016/j.quascirev.2006.04.012.
443   47.   Glennie, K.W.; Singhvi, A.K. Event stratigraphy, paleoenvironment and chronology of SE Arabian deserts.
444         *Quat. Sci. Rev.* **2002**, *21*, 853–869. DOI:10.1016/S0277-3791(01)00133-0.
445   48.   Parker, A.G.; Goudie, A.S. Geomorphological and palaeoenvironmental investigations in the southeastern
446         Arabian Gulf region and the implication for the archaeology of the region. *Geomorphology* **2008**, *101*, 458–
447         470, DOI:10.1016/j.geomorph.2007.04.028.
448   49.   Engel, M.; Brückner, H.; Pint, A.; Wellbrock, K.; Ginau, A.; Voss, P.; Grottker, M.; Klasen, N.; Frenzel, P.
449         The early Holocene humid period in NW Saudi Arabia — sediments, microfossils and palaeohydrological
450         modelling. *Quat. Int.* **2012**, *266*, 131–141, DOI:10.1016/j.quaint.2011.04.028.
451   50.   Matter, A.; Neubert, E.; Preusser, F.; Rosenberg, T.; Al-Wagdani, K. Palaeo-environmental implications
452         derived from lake and sabkha deposits of the southern Rub'al-Khali, Saudi Arabia and Oman. *Quat. Int.*
453         **2015**, *382*, 120–131, DOI:10.1016/j.quaint.2014.12.029.
454   51.   Lancaster, N.; Baas, A. Influence of vegetation cover on sand transport by wind: field studies at Owens
455         Lake, California. *Earth Surf. Process. Landforms* **1998**, *23*, 69–82, DOI:10.1002/(SICI)1096-
456         9837(199801)23:1<69::AID-ESP823>3.0.CO;2-G.
457   52.   Thomas, D.S.G.; Knight, M.; Wiggs, G.F.S. Remobilization of southern African desert dune systems by
458         twenty-first century global warming. *Nature* **2005**, *435*, 1218–1221, DOI:10.1038/nature03717.
459   53.   Yizhaq, H.; Ashkenazy, Y.; Tsoar, H. Sand dune dynamics and climate change: A modeling approach. *J.*
460         *Geophys. Res.* **2009**, *114*, F01023, DOI:10.1029/2008JF001138.
461   54.   Gillette D.A.; Adams J. Accelerated Wind Erosion and Prediction of Rates. In *Environmental Effects of Off-*
462         *Road Vehicles*; Webb, R.H., Wilshire H.G., Eds; Springer, New York, USA, 1983; pp. 97–111, DOI:10.1007/978-
463         1-4612-5454-6_6.